A Practical Approach to the Design of Long Sandwich Plates

 Erkin Altunsaray, Gökdeniz Neşer

Dokuz Eylül University, Institute of Marine Sciences and Technology, Department of Naval Architecture, İzmir, Türkiye

Abstract

Sandwich materials in plate form, crafted from advanced composite face sheets and lightweight core materials, are extensively utilized in marine structures, particularly in pleasure boats. This is due to their high specific strength, ease of formability, high rigidity, and cost-effectiveness. Given their complex internal structures, there is a pressing need for practical methods to accurately analyze the behavior of sandwich plates during the preliminary design phase, where time constraints can heavily impact the designer's decisions. Although rule-based approaches are often seen as a quick and suitable solution for reaching initial design assumptions, they can result in heavier structures compared to those achieved through optimization using more time-intensive numerical methods, ultimately leading to suboptimal designs. This study presents a practical method for obtaining a lightweight sandwich structure without the necessity of numerical analyses, utilizing a parametric approach specifically developed for this purpose. The approach is tailored to address the design of a sandwich plate representing the bottom of a boat. It features carbon fiber-reinforced epoxy face sheets and a PVC foam core, which is simply supported at the edges while being subjected to compressive loads that can induce buckling along the long edges. Ansys was also used to select the lightest one among 12 different sandwich plate combinations. The optimization was carried out on the basis of critical buckling loads obtained by the Long Sandwich Plate Method.

Keywords: Critical buckling load, Long Sandwich Plate Method (LSPM), structural optimization, ship structural analysis

1. Introduction

Sandwich plate materials made from polymer-based composites are extensively used in the marine industry, serving various purposes, from the hull structures of ships to their components. These plates are utilized by ships and in structures that generate marine renewable energy, such as wind turbines and wave energy converters, as well as in modern technologies like unmanned marine vehicles [1-6]. These materials have proven to be an excellent choice due to their superior specific strength, meaning they are lightweight while maintaining high strength. Additionally, they offer advantages in logistics and production with low emissions and have a long lifespan primarily because of their resistance to environmental factors. This aligns well with current environmental concerns that drive industries toward sustainability in design and production. Other benefits of sandwich structures in marine applications include good buckling resistance and crashworthiness, reduced construction weight, and the ability to support large spans without additional stiffening. This results in increased usable volume, greater design flexibility, fewer parts, and reduced assembly time. The marine industry can widely use sandwich materials made from polymer-based composites. This includes innovative applications that ensure time-saving designs and allow designers to work freely. Because

Address for Correspondence: Erkin Altunsaray, Dokuz Eylül University Institute of Marine Sciences and Technology, Department of Naval Architecture, İzmir, Türkiye

E-mail: erkin.altunsaray@deu.edu.tr
ORCID ID: orcid.org/0000-0003-3099-6059

these materials can easily produce complex forms that cannot be achieved with metal or alloy equivalents, this flexibility in design allows for innovative shapes and structures that can enhance performance and aesthetic appeal. Glass or carbon fiber-reinforced epoxy or vinyl ester composites are commonly used as face sheets. At the same time, closed or open-cell foam, balsa of various densities, and aluminum honeycombs serve as cores. These materials are notable components of sandwich structures made from polymer-based composites, which are widely utilized in the boatbuilding industry.

The loads that the structural elements of ships, especially those sailing in rough seas, must carry are quite variable in terms of their magnitude, the direction of action (compression, tension, shear, compound, bending, torsion, buckling, etc.), and behavior (cyclic, randomly variable over time, singular, shock, etc.). The selection and dimensioning of the materials of the structural elements are made by taking into account the various loads that a ship in the design phase may encounter throughout its life. In marine conditions, buckling comes to the forefront as the inevitable load that elements in plate form will be exposed to.

Research on buckling, recognized as the most critical load that sandwich plates encounter, focuses on optimizing both the geometry and lamination of these plates under the relevant loads [7-9] and selecting the appropriate materials. When addressing complex challenges, such as designing the bottom sandwich plates of high-speed marine vehicles, buckling loads are typically analyzed using various plate theories, considering them as uniformly distributed axial and biaxial in-plane loads [10,11].

It is worth noting that the first scientific publication on sandwich plates was a study by Marquerre in 1944 on the behavior of these structures under buckling loads, which was cited in [12]. Most research investigating the buckling behavior of sandwich composite plates focuses on enhancing the mechanical properties of the facesheet and core components by using auxiliary materials, such as modifications with multi-walled carbon nanotubes [13-15]. Additionally, at an analytical level, studies that aim to determine buckling responses utilize approaches like Reddy's higher-order shear deformation theory [16] as well as numerical methods, including the Finite Element Method (FEM) and the Generalized Differential Quadrature Method [17].

In this study, the optimization of the components (face sheets and core) of rectangular sandwich plates with long length compared to their width and subjected to buckling load, representing the bottom structure of a small marine craft, was carried out with the Long Sandwich Plate Method (LSPM)

[18,19]. The obtained analytical results were also verified with the help of the ANSYS software [20] based on the FEM. The study aims to propose practical tools for designers who design composite sandwich plates, whose numerical or analytical modeling requires expertise and time, such as the graph that gives the critical buckling loads depending on the plate dimensions presented at the end.

2. Materials and Methods

2.1. Governing Equations of Sandwich Plates Under Critical Buckling Load

Kirchhoff Plate Theory is applied to analyze thin plates undergoing small deformations. Under this theory, it is assumed that after deformation, the normal to the plane remains perpendicular to the reference plane and does not curve. The governing equations for plates and thin plates are presented below.

In the case of sandwich plates, the normal line remains straight but is not perpendicular to the reference plates (neutral axis) (Figure 1). The displacements at the x and y axis are given in Equation 1.

$$u = u^0 - z\chi_{xz} \quad v = v^0 - z\chi_{yz} \qquad (1)$$

where, χ_{xz} and χ_{yz} are the rotations of the normals at the x-z and y-z planes, respectively.

From Figure 1, the first derivative of the deflection w^0 of reference plane with respect to x is

$$\frac{\partial w^0}{\partial x} = \chi_{xz} + \gamma_{xz} \qquad (2)$$

and similarly the first derivative of the w^0 of reference plane with respect to y is,
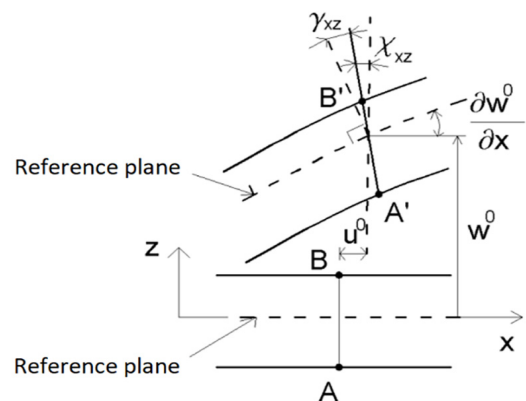

Figure 1. Deformation of a sandwich plates [18]

$$\frac{\partial w^0}{\partial y} = \chi_{yz} + \gamma_{yz} \tag{3}$$

As for the strains at the reference planes are,

$$\epsilon_x^0 = \frac{\partial u^0}{\partial x} \quad , \quad \epsilon_y^0 = \frac{\partial v^0}{\partial y} , \quad \gamma_{xy}^0 = \frac{\partial u^0}{\partial y} + \frac{\partial v^0}{\partial x} \tag{4}$$

From Equations 2 and 3, transverse shear strains are

$$\gamma_{xz} = \frac{\partial w^0}{\partial x} - \chi_{xz} , \quad \gamma_{yz} = \frac{\partial w^0}{\partial y} - \chi_{yz} \tag{5}$$

While shear deformation is zero, those expressions of curvatures of reference planes can be reached

$$\kappa_x = -\frac{\partial \chi_{xz}}{\partial x}, \quad \kappa_y = -\frac{\partial \chi_{yz}}{\partial y}, \quad \kappa_{xy} = -\frac{\partial \chi_{xz}}{\partial y} - \frac{\partial \chi_{yz}}{\partial x} \tag{6}$$

From these Equations 4-6, strain-displacement relations of the sandwich plates can be seen.

The section of the sandwich plate is illustrated in Figure 2, where t^t and t^b represent the thicknesses of the outer and inner (upper and lower) face sheets, respectively. In this study, t^t and t^b are equal, as they share the same thickness and symmetrical lamination sequence. Similarly, the reference plane is located at the midplane of the sandwich plate, which means that d^t and d^b are also equal. For these variables, the relationship d=c+t is shown in Figure 2.

To establish the force-strain relationship, the forces and moments are described in Equations 7 and 8, respectively.

$$N_x = \int_{-h_b}^{h_t} \sigma_x dz , \quad N_y = \int_{-h_b}^{h_t} \sigma_y dz,$$

$$N_{xy} = \int_{-h_b}^{h_t} \tau_{xy} dz , \quad M_x = \int_{-h_b}^{h_t} z\sigma_x dz, \tag{7}$$

$$M_y = \int_{-h_b}^{h_t} z\sigma_y dz, \quad M_{xy} = \int_{-h_b}^{h_t} z\tau_{xy} dz$$

$$V_x = \int_{-h_b}^{h_t} \tau_{xz} dz , \quad V_y = \int_{-h_b}^{h_t} \tau_{yz} dz \tag{8}$$

N_i, M_i, and V_i are in plane forces, moments and transverse shear forces respectively. h_t and h_b are the distances from the reference plane to the surface of the plate.
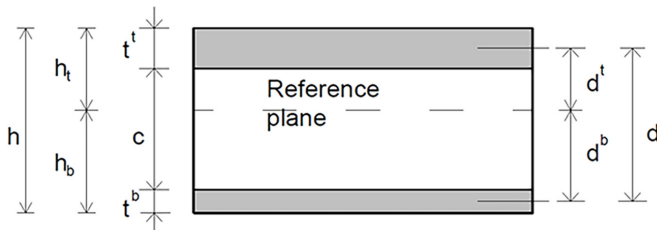

Figure 2. Sandwich plate geometry [18]

As for in-plane stresses,

$$\begin{Bmatrix} \sigma_x \\ \sigma_y \\ \tau_{xy} \end{Bmatrix} = \begin{bmatrix} \overline{Q}_{11} & \overline{Q}_{12} & \overline{Q}_{16} \\ \overline{Q}_{12} & \overline{Q}_{22} & \overline{Q}_{26} \\ \overline{Q}_{16} & \overline{Q}_{26} & \overline{Q}_{66} \end{bmatrix} \begin{Bmatrix} \epsilon_x \\ \epsilon_y \\ \gamma_{xy} \end{Bmatrix} \tag{9}$$

As for the strains at z distance from the reference plane:

$$\epsilon_x = \frac{\partial u}{\partial x} = \frac{\partial u^0}{\partial x} - z\frac{\partial \chi_{xz}}{\partial x}$$

$$\epsilon_y^0 = \frac{\partial v}{\partial y} = \frac{\partial v^0}{\partial y} - z\frac{\partial \chi_{yz}}{\partial y} \tag{10}$$

$$\gamma_{xy}^0 = \frac{\partial u}{\partial y} + \frac{\partial v}{\partial x} = \frac{\partial u^0}{\partial y} + \frac{\partial v^0}{\partial x} - z\left(\frac{\partial \chi_{xz}}{\partial y} + \frac{\partial \chi_{yz}}{\partial x}\right)$$

From the Equations 4th, 7th, 9th and 10th and the definitions of rigidity matrices [A], [B] and [D], following expressions can be obtained:

$$\begin{Bmatrix} N_x \\ N_y \\ N_{xy} \end{Bmatrix} = [A]\begin{Bmatrix} \epsilon_x^0 \\ \epsilon_x^0 \\ \gamma_{xy}^0 \end{Bmatrix} + [B]\begin{Bmatrix} -\frac{\partial \chi_{xz}}{\partial x} \\ -\frac{\partial \chi_{yz}}{\partial y} \\ -\frac{\partial \chi_{xz}}{\partial y} - \frac{\partial \chi_{yz}}{\partial x} \end{Bmatrix} \tag{11}$$

$$\begin{Bmatrix} M_x \\ M_y \\ M_{xy} \end{Bmatrix} = [B]\begin{Bmatrix} \epsilon_x^0 \\ \epsilon_x^0 \\ \gamma_{xy}^0 \end{Bmatrix} + [D]\begin{Bmatrix} -\frac{\partial \chi_{xz}}{\partial x} \\ -\frac{\partial \chi_{yz}}{\partial y} \\ -\frac{\partial \chi_{xz}}{\partial y} - \frac{\partial \chi_{yz}}{\partial x} \end{Bmatrix} \tag{12}$$

From the Equation 6, the Equations 11 and 12 can be written as;

$$\begin{Bmatrix} N_x \\ N_y \\ N_{xy} \end{Bmatrix} = [A]\begin{Bmatrix} \epsilon_x^0 \\ \epsilon_x^0 \\ \gamma_{xy}^0 \end{Bmatrix} + [B]\begin{Bmatrix} \kappa_x \\ \kappa_y \\ \kappa_{xy} \end{Bmatrix} \tag{13}$$

$$\begin{Bmatrix} M_x \\ M_y \\ M_{xy} \end{Bmatrix} = [B]\begin{Bmatrix} \epsilon_x^0 \\ \epsilon_x^0 \\ \gamma_{xy}^0 \end{Bmatrix} + [D]\begin{Bmatrix} \kappa_x \\ \kappa_y \\ \kappa_{xy} \end{Bmatrix} \tag{14}$$

The relation between transverse shear forces and transverse shear stress can be given as,

$$\begin{Bmatrix} V_x \\ V_y \end{Bmatrix} = \begin{bmatrix} \breve{S}_{11} & \breve{S}_{12} \\ \breve{S}_{12} & \breve{S}_{22} \end{bmatrix} \begin{Bmatrix} \gamma_{xz} \\ \gamma_{yz} \end{Bmatrix} \tag{15}$$

J Nav Architect Mar Technol
2024;226(2):80-90

Altunsaray and Neşer.
A Practical Approach to the Design of Long Sandwich Plates

where $[\breve{S}]$ is the shear stiffness matrix (rigidity matrix) of the sandwich plate.

At the boundary conditions for simple support, deflection, w^0, boundary moment, M_x, torsion moment M_{xy}, and in-plane forces N_x and N_{xy} are zero.

$$w^0 = 0, \; M_x = M_{xy} = 0, \; N_x = N_{xy} = 0 \tag{16}$$

so, governing equations of thin plates can be given below

Force-strain relations:

$$\begin{Bmatrix} N_x \\ N_y \\ N_{xy} \\ M_x \\ M_y \\ M_{xy} \end{Bmatrix} = \begin{bmatrix} A_{11} & A_{12} & A_{16} & B_{11} & B_{12} & B_{16} \\ A_{12} & A_{22} & A_{26} & B_{12} & B_{22} & B_{26} \\ A_{16} & A_{26} & A_{66} & B_{16} & B_{26} & B_{66} \\ B_{11} & B_{12} & B_{16} & D_{11} & D_{12} & D_{16} \\ B_{12} & B_{22} & B_{26} & D_{12} & D_{22} & D_{26} \\ B_{16} & B_{26} & B_{66} & D_{16} & D_{26} & D_{66} \end{bmatrix} \begin{Bmatrix} \epsilon_{lx}^0 \\ \epsilon_y^0 \\ \gamma_{xy}^0 \\ \kappa_x \\ \kappa_y \\ \kappa_{xy} \end{Bmatrix} \tag{17}$$

A_{ij}, B_{ij}, and D_{ij} in Equation 17th are the extensional, Aijbending-extension coupling, and bending stiffnesses matrices, respectively. These matrices are shown in the form of reduced stiffness matrices below,

$$A_{ij} = \sum_{k=1}^{K} \left(\overline{Q}_{ij} \right)_k (z_k - z_{k-1})$$

$$B_{ij} = \frac{1}{2} \sum_{k=1}^{K} \left(\overline{Q}_{ij} \right)_k (z_k^2 - z_{k-1}^2) \tag{18}$$

$$D_{ij} = \frac{1}{3} \sum_{k=1}^{K} \left(\overline{Q}_{ij} \right)_k (z_k^3 - z_{k-1}^3)$$

The elements of the reduced stiffness matrix of $\left[\overline{Q} \right]$ are given below:

$$\overline{Q}_{11} = c^4 Q_{11} + s^4 Q_{22} + 2c^2 s^2 \left(Q_{12} + 2Q_{66} \right)$$

$$\overline{Q}_{22} = s^4 Q_{11} + c^4 Q_{22} + 2c^2 s^2 \left(Q_{12} + 2Q_{66} \right)$$

$$\overline{Q}_{12} = c^2 s^2 \left(Q_{11} + Q_{22} - 4Q_{66} \right) + \left(c^4 + s^4 \right) Q_{12}$$

$$\overline{Q}_{66} = c^2 s^2 \left(Q_{11} + Q_{22} - 2Q_{12} \right) + \left(c^2 - s^2 \right)^2 Q_{66} \tag{19}$$

$$\overline{Q}_{16} = cs \left(c^2 Q_{11} - s^2 Q_{22} - \left(c^2 - s^2 \right)\left(Q_{12} + 2Q_{66} \right) \right)$$

$$\overline{Q}_{26} = cs \left(s^2 Q_{11} - c^2 Q_{22} + \left(c^2 - s^2 \right)\left(Q_{12} + 2Q_{66} \right) \right)$$

Here $c = \cos\theta$ and $s = \sin\theta$.

To determine the stiffness matrix of the sandwich plate, the following procedure will be used:

It is assumed that the thickness of the core is constant and in-plane stiffnesses of the core are neglected. By these assumptions, the stiffness matrices [A], [B], and [D] can be obtained by using the stiffnesses of face sheets and parallel axes theorem.

Since the upper and lower facesheets are the same and have a symmetrical lamination sequence to their midplane, the bending-extension coupling stiffness matrix, [B], is zero while the bending-extension coupling matrix, [A], is the summation of the upper and lower extensional matrices.

$$[A] = 2[A]^t \tag{20}$$

and [D] is the bending stiffness matrix,

$$[D] = \frac{1}{2} d^2 [A]^t + 2[D]^t \tag{21}$$

To determine the shear rigidity matrix, $[\breve{S}]$, the transverse shear stresses, τxz are distributed uniformly due to the assumption of neglecting in-plane stiffness of cores. Generally, the shear stress distribution of outer face sheets is like that shown in Figure 3a. This approach assumes a linear shear stress distribution (Figure 3b). Accordingly, the transverse shear force, V_x is

$$V_x = \int_{-h_b}^{h_b} \tau_{xz} \, dz = \tau_{xz}^c + \tau_{xz}^c \frac{t^t}{2} + \tau_{xz}^c \frac{t^b}{2} = \tau_{xz}^c d \tag{22}$$

and

$$d = c + \frac{t^t}{2} + \frac{t^b}{2} \tag{23}$$

where the relations c, t, and b are core, outer (upper), and inner (lower) face sheets, respectively, while d is given in Figure 3.

Similarly, V_y is given below,

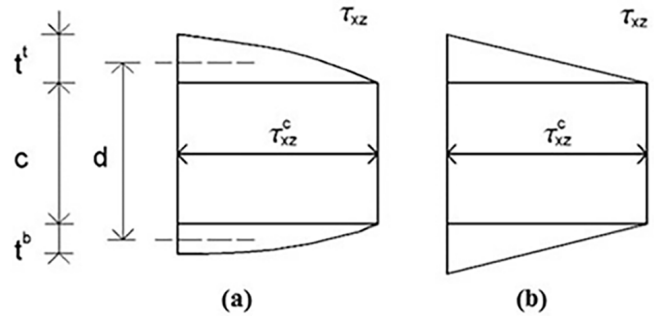$$V_y = \tau_{yz}^c d \tag{24}$$

Figure 3. (a) Actual distribution, (b) approximate distribution of shear stress at the sandwich plate [18]

The relation between stress and strain in the core material is also given below.

$$\begin{Bmatrix} \tau^c_{xz} \\ \tau^c_{yz} \end{Bmatrix} = \begin{bmatrix} \overline{C}^c_{55} & \overline{C}^c_{45} \\ \overline{C}^c_{45} & \overline{C}^c_{44} \end{bmatrix} \begin{Bmatrix} \gamma^c_{xz} \\ \gamma^c_{yz} \end{Bmatrix} \tag{25}$$

Where $\overline{C}^c_{ij}$ is the element of the stiffness matrix of the core. In Equation 25, the shear deformations of the outer face sheets are neglected. By this approach, the transverse section of γ^c_{xz} is shown in Figure 4a. The mean shear deformation, γ_{xz} is also shown in the Figure 4b. As for Figure 4c. shows the relation between shear deformation and core deformation.

From Figure 4,

$$\gamma^c_{xz} = \frac{d}{c}\gamma_{xz}, \gamma^c_{yz} = \frac{d}{c}\gamma_{yz} \tag{26}$$

From the Equations 22-26, the relation between transverse shear forces and mean shear deformations yields:

$$\begin{Bmatrix} V_x \\ V_y \end{Bmatrix} = \frac{d^2}{c}\begin{bmatrix} \overline{C}^c_{55} & \overline{C}^c_{45} \\ \overline{C}^c_{45} & \overline{C}^c_{44} \end{bmatrix} \begin{Bmatrix} \gamma_{xz} \\ \gamma_{yz} \end{Bmatrix} \tag{27}$$

By substituting the Equation 15 into Equation 27:

$$\begin{bmatrix} \widetilde{S}_{11} & \widetilde{S}_{12} \\ \widetilde{S}_{12} & \widetilde{S}_{22} \end{bmatrix} = \frac{d^2}{c}\begin{bmatrix} \overline{C}^c_{55} & \overline{C}^c_{45} \\ \overline{C}^c_{45} & \overline{C}^c_{44} \end{bmatrix} \tag{28}$$

2.2. Buckling of Long Sandwich Plates

Long rectangular plates have length, b is quite larger compared to its width a ($b \gg a$). The boundary condition is simply supported at the edges of the plate. A uniform compressive force N_{x0} is applied along the long edges of the plate. The deflected surface of the plate can be assumed to be cylindrical at a significant distance from the short edges and is parallel to the axis.

The LPSM can be applied for orthotropic plates when the following inequality is satisfied [18]:

$$\frac{b}{a} > 3\sqrt[4]{\frac{D_{11}}{D_{22}}} \tag{29}$$

Where D_{11} and D_{22} are bending stiffness matrix elements. The equilibrium equations are given below

$$\frac{dV_x}{dx} - N_{x0}\frac{d^2w^0}{dx^2} = 0 \tag{30}$$

$$\frac{dM_x}{dx} - V_x = 0 \tag{31}$$

The sandwich plate is symmetrical to the midplane. The bending moment and the transverse shear force are given below

$$M_x = -D_{11}\frac{\partial \chi_{xz}}{\partial x}, V_x = \widetilde{S}_{11}\gamma_{xz} \tag{32}$$

From the Equations 30, 31, 32, and 2, the expressions of symmetrically laminated plates

$$-D_{11}\frac{d^3\chi}{dx^3} - N_{x0}\frac{d^2w^0}{dx^2} = 0 \tag{33}$$

$$D_{11}\frac{d^2\chi}{dx^2} + \widetilde{S}_{11}\left(\frac{dw^0}{dx} - \chi\right) = 0 \tag{34}$$

As for isotropic sandwich plates

$$-\widehat{EI}\frac{d^3\chi}{dx^3} - \widehat{N}_{x0}\frac{d^2w^0}{dx^2} = 0 \tag{35}$$

$$\widehat{EI}\frac{d^2\chi}{dx^2} + \widehat{S}\left(\frac{dw}{dx} - \chi\right) = 0 \tag{36}$$

where $\widehat{EI}$ and $\widehat{S}$ are the bending and shear stiffnesses, respectively, and $\widehat{N}_{x0}$ is the compressive load acting on the length of the plate.
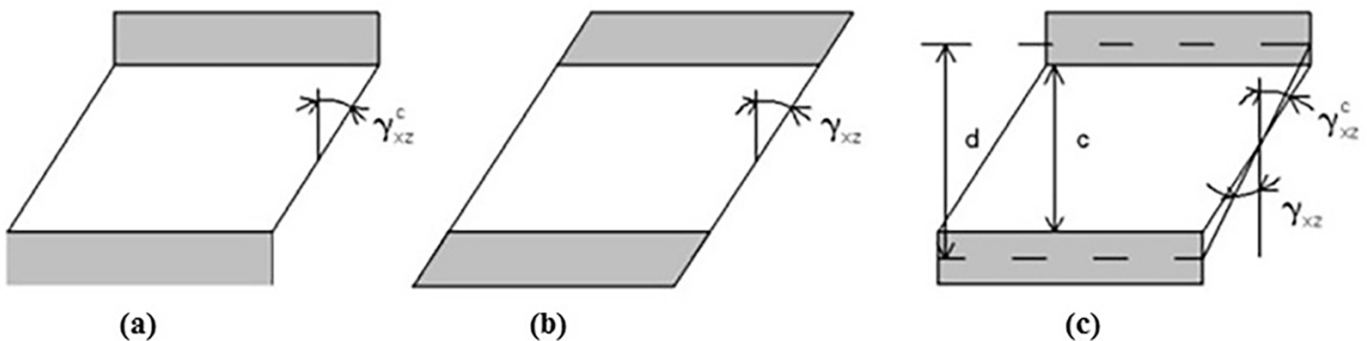

Figure 4. (a-c) Shear deformations of a sandwich plate [18]

By substituting D_{11}, $\tilde{S}_{11}$, and $\hat{N}_{x0}$ of the Equations 35 and 36 into $\widehat{EI}$, $\hat{S}$, and $\hat{N}_{x0}$, the buckling equation of by sandwich plates was obtained.

The critical buckling load of an isotropic sandwich beam for the simply supported boundary condition is given below:

$$\widehat{N_{cr}} = \left(\frac{a^2}{\pi^2 E I} + \frac{1}{\hat{S}} \right)^{-1} \tag{37}$$

The critical buckling load of a symmetrical laminated long sandwich plate for the simply supported boundary condition is given below

$$N_{x,cr} = \left(\frac{a^2}{\pi^2 D_{11}} + \frac{1}{\tilde{S}_{11}} \right)^{-1} \tag{38}$$

The shear stiffness matrix is given below

$$\begin{bmatrix} \tilde{S}_{11} & \tilde{S}_{12} \\ \tilde{S}_{12} & \tilde{S}_{22} \end{bmatrix} = \frac{d^2}{c} \begin{bmatrix} \overline{C}^c_{55} & \overline{C}^c_{45} \\ \overline{C}^c_{45} & \overline{C}^c_{44} \end{bmatrix} \tag{39}$$

where

$$\overline{C}^c_{55} = \overline{C}^c_{44} = \frac{E}{2(1 + \nu)}, \overline{C}^c_{45} = 0 \tag{40}$$

for isotropic core material.

2.3. Sandwich Plate Forms, their Laminates, and Properties

The sandwich plates under investigation are illustrated in Figure 5, which includes the coordinate system used for analysis, as well as the dimensions of the short edge (a) and long edge (b) of the plates, their thickness, and the direction of the applied buckling load. The face sheets of these plates are made from symmetrically laminated, quasi-isotropic carbon fiber-reinforced epoxy composites, while the core

material consists of PVC foam with varying densities. Notably, the long edge of the rectangular plate, referred to as 'b' in this study, is significantly longer than the short edge, designated as "a".

The properties of the components of 12 diferent sandwich panels are given in Table 1.

Some other specific properties (such as lamination sequences, core, and face sheet thicknesses) of twelve different sandwich plates considered in this study are given in Table 2. While laminating the face sheets of the plates, the carbon fibers were placed in three different directions, 0º, 45º, and 90º.

2.4. Numerical Approach

A commercial software application based on the FEM was used to calculate the critical buckling loads. The results obtained from this software were compared with those derived from the LSPM. In the numerical model, a rectangular four-point shell element was selected (refer to Figure 6). A square mesh with a size of 1/20 of the short edge of the sandwich
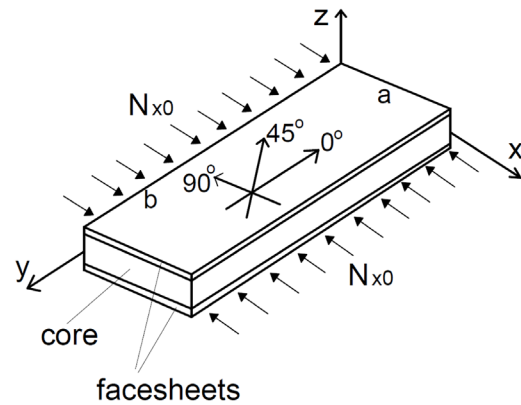

Figure 5. Form of sandwich plate studied and its buckling loads exposed

Table 1. Material properties							
Facesheets (carbon/epoxy, T300-934) [18]							
Longitudinal Young's Modulus (E_{11}) (GPa)	148						
Transverse Young's Modulus (E_{22}) (GPa)	9.65						
Longitudinal Shear Modulus (G_{12}) (GPa)	4.55						
Longitudinal Poisson ratio (ν_{12})	0.3						
Lamina thickness (t) (m)	0.1×10^{-3}						
Density ($\rho0$) (kg/m³)	1.5×10^3						
Core (PVC foam) [21]							
	H45	H60	H80	H100	H130	H160	H200	H250
Young's Modulus (E) (MPa)	55	75	95	130	175	205	250	320
Density ($\rho0$) (kg/m³)	48	60	80	100	130	160	200	250
Poisson ratio (ν)	0.4							

Altunsaray and Neşer.
A Practical Approach to the Design of Long Sandwich Plates

J Nav Architect Mar Technol
2024;226(2):80-90

Table 2. Sandwich plate studied LSPM

| Plate no | Facesheets | | | | Core | | | a (m) | b (m) | Plate | | Bending stiffness values | | LSPM |
	The arrangement of layers on either side of the axis of symmetry	Thickness (mm)	Density (kg/m³)	Weight (gr)	Thickness (mm)	Weight (gr)	Density (kg/m³)			Weight (gr)	Density (kg/m³)	D_{11} (N.m)	D_{22} (N.m)	$\frac{b}{a} > 3 \quad \sqrt[4]{\frac{D_{11}}{D_{22}}}$
1	[90/-45/45/0]	1.6	1500	298	10	124	100	0.2	0.62	422	293	2916.9	2923.6	3.1 >2.9983
2	[902/-452/452/02]	3.2	1500	595	10	124	100	0.2	0.62	719	439	6742.9	6796.4	3.1 >2.9941
3	[903/-453/453/03]	4.8	1500	893	10	124	100	0.2	0.62	1017	554	11588	11768	3.1 >2.9884
4	[90/-45/45/0]	1.6	1500	298	5	62	100	0.2	0.62	360	439	842.8	849.5	3.1 >2.9941
5	[90/-45/45/0]	1.6	1500	298	15	186	100	0.2	0.62	484	235	6240.3	6247	3.1 >2.9992
6	[-452/452/902/02]	2.3	1500	595	10	124	100	0.2	0.62	719	439	6754.4	6763.3	3.1 >2.9990
7	[452/02/-452/902]	2.3	1500	595	10	124	100	0.2	0.62	719	439	6776.6	6749.8	3.1 >3.0030
8	[02/-452/452/902]	2.3	1500	595	10	124	100	0.2	0.62	719	439	6796.4	6742.9	3.1 >3.0059
9	[90/-45/45/0]	1.6	1500	298	34	421	100	0.2	0.62	719	163	3026.4	3027.1	3.1 >2.9998
10	[-45/45/90/0]	1.6	1500	298	34	421	100	0.2	0.62	719	163	3-026.6	3026.7	3.1 >3.0000
11	[45/0/-45/90]	1.6	1500	298	34	421	100	0.2	0.62	719	163	3026.8	3026.5	3.1 >3.0001
12	[0/-45/45/90]	1.6	1500	298	34	421	100	0.2	0.62	719	163	3027.1	3026.4	3.1 >3.0002

plate was employed. This element operates according to First Order Shear Deformation Theory, specifically the Mindlin-Reissner Shell Theory.

3. Results and discussions

In this study, the critical buckling loads were determined using LSPM and FEM-based numerical modeling. The related results are presented comparatively in Figure 7. $\tilde{S}_{11}$ was obtained using Equation 39 since the E is Young modulus of core, and v is Poisson ratios of core the only variable parameter in the calculation was D_{11}, which was derived from Equation 21. In this equation, d is a function of plate thickness, (A) is the extensional stiffness matrix of face sheets, and (D) is the bending stiffness matrix of face sheets. In long sandwich plates, the critical buckling value increases with the increase of the plate thickness and the elements of the A and D matrix.

Figure 7 shows that as the core thickness increases, the critical buckling load increases, as expected. Sandwich plates with thick core material have lower density but higher strength. In fact, a three-fold increase in core thickness increases the specific strength (load/density) based on the critical buckling load by 10 times.

The results clearly showed that at Plate 4, whose core thickness is the lowest, has the lowest critical buckling load. Since the plate has a thinner core (5 mm), it behaved as a single skin rather than a sandwich plate. This phenomenon also shows that the core thickness should be larger than a certain value. Without considering Plate no. 4, the results were very well fitted to a cubic polynomial given in Figure 8.

The results also showed that the critical buckling loads were independent of the rate of the aspect ratio (b/a) of the plates when it is larger than b/a=3.0. Almost the same results were found for b/a=3.1 and 4.0 (Figure 9).

The graph of the critical buckling loads that sandwich plates can withstand depending on their densities by changing the core materials is presented in Figure 10. In this graph, plate number 4, which was seen to be a single skin plate rather than a sandwich plate, was not taken into account. According to this figure, critical density range should be considered when designing sandwich plates. An approach that designers will use when choosing the right core materials is suggested in this graph. Namely, when designing a sandwich material, it is seen that it should prefer cores with a density of less than 300 kg.m^{-3} and more than 400 kg.m^{-3}.
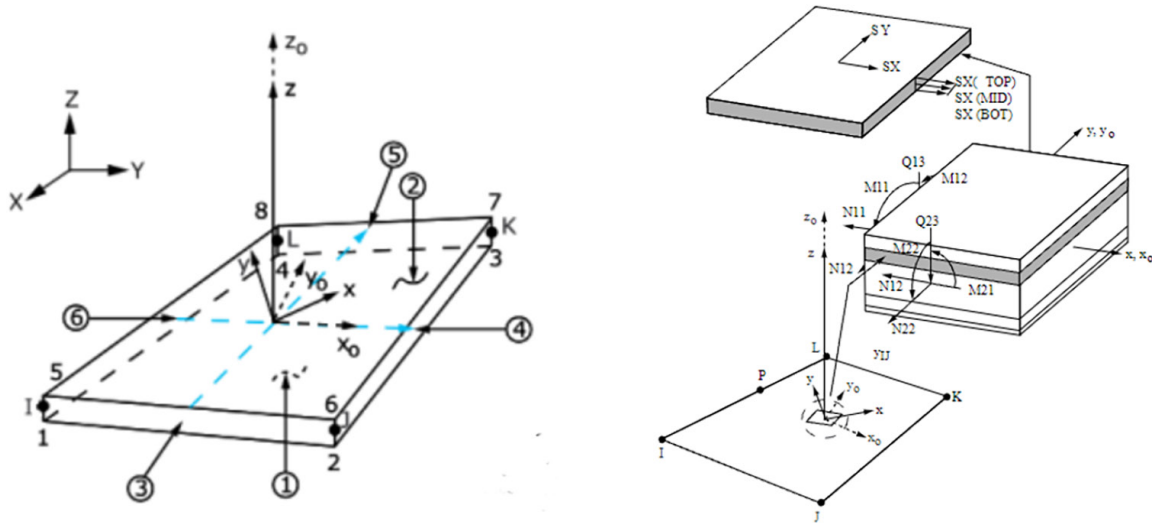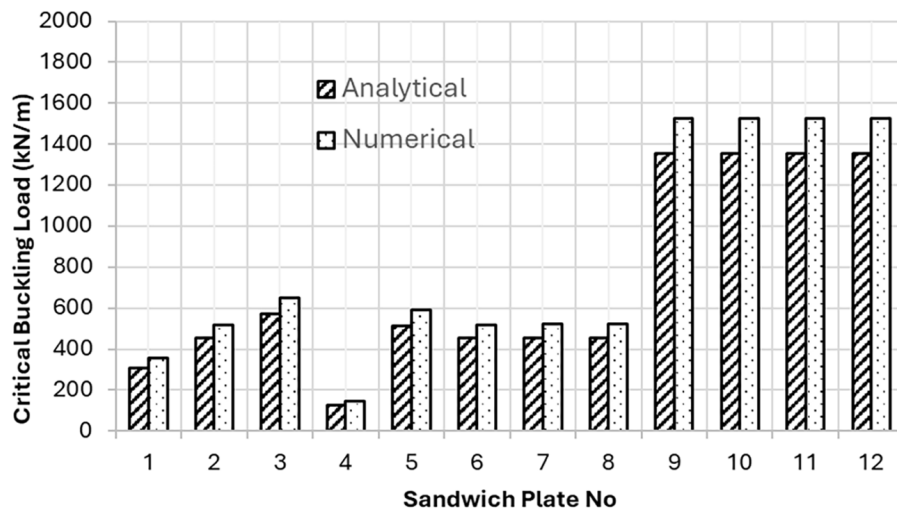
Figure 6. SHELL 181 element (ANSYS)

Figure 7. Critical buckling load of sandwich plates

In a comparison of eight sandwich plates with different face sheets and core materials, it was also found that there were no significant effects of lamination sequences on the critical buckling loads. It is also seen that sandwiches designed with thinner face sheets and thicker cores can carry higher critical buckling loads.

4. Conclusion

This study proposes a practical method to assist sandwich material designers based on the critical buckling load. This load is obtained both numerically (using the Ansys software based on the FEM) and analytically (using LSPM), which validate each other.

Critical buckling loads were systematically obtained for 88 plate combinations consisting of different core and face sheets. These plates were assumed simply supported at their four edges and subjected to axial compression loads along their long edges.

It has also been observed that the face sheets and edge dimensions of the sandwich plate are not effective in forming the critical buckling load. However, the thickness of the core material is more decisive as the lowest-density sandwich plate component. In practice, designers should choose this core thickness to give the plate a sandwich character and reduce the density.
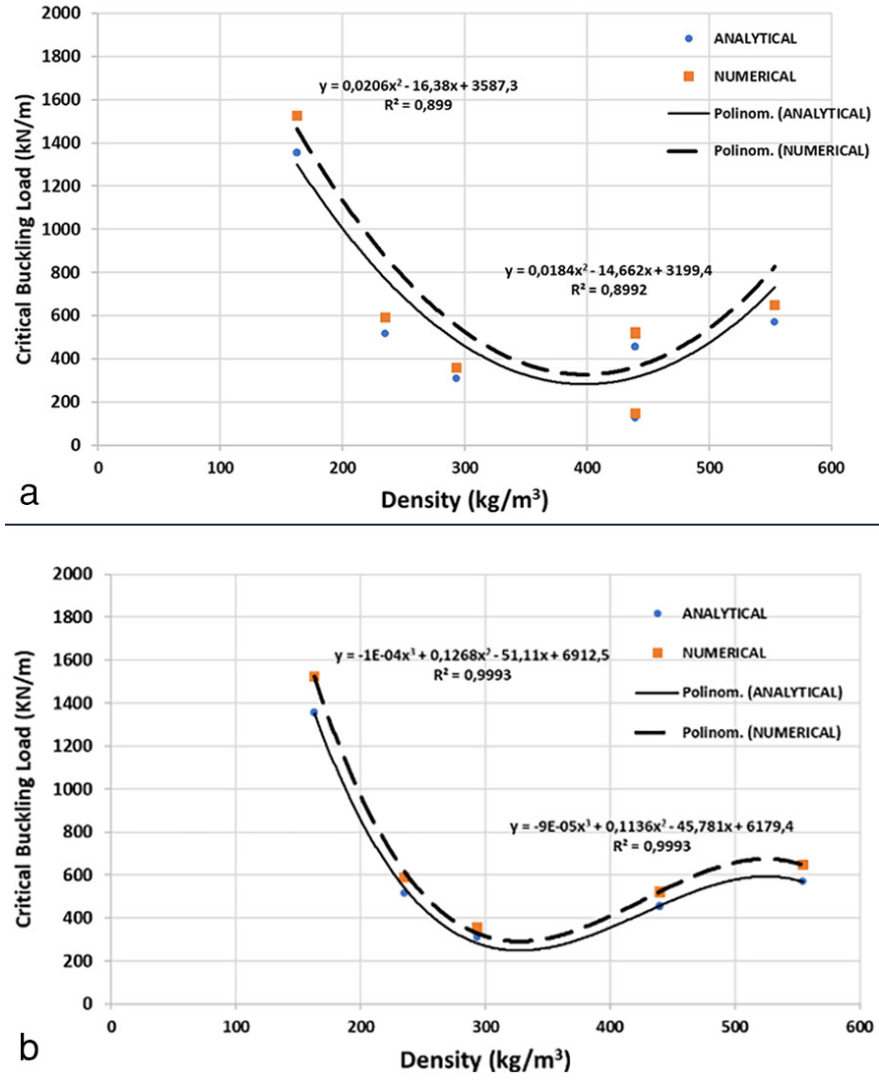
Figure 8. Critical buckling load versus density with (**a**) and without (**b**) Plate no. 4
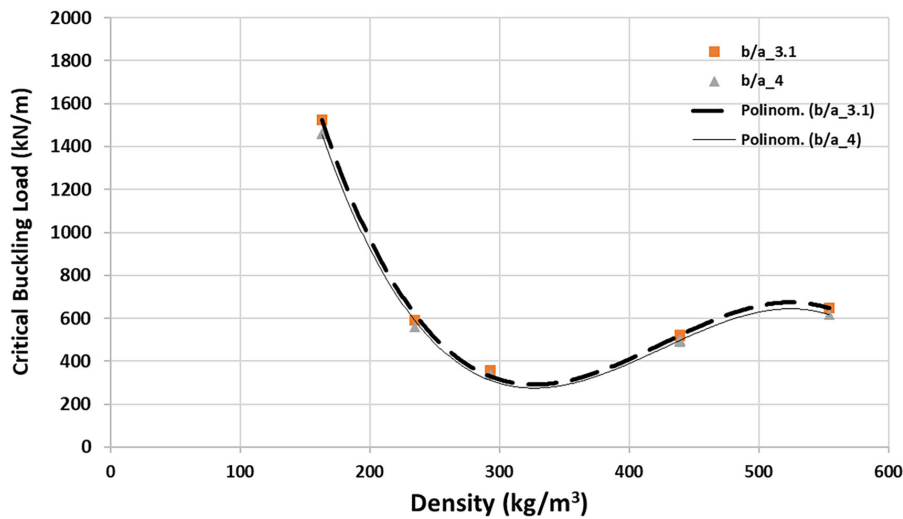

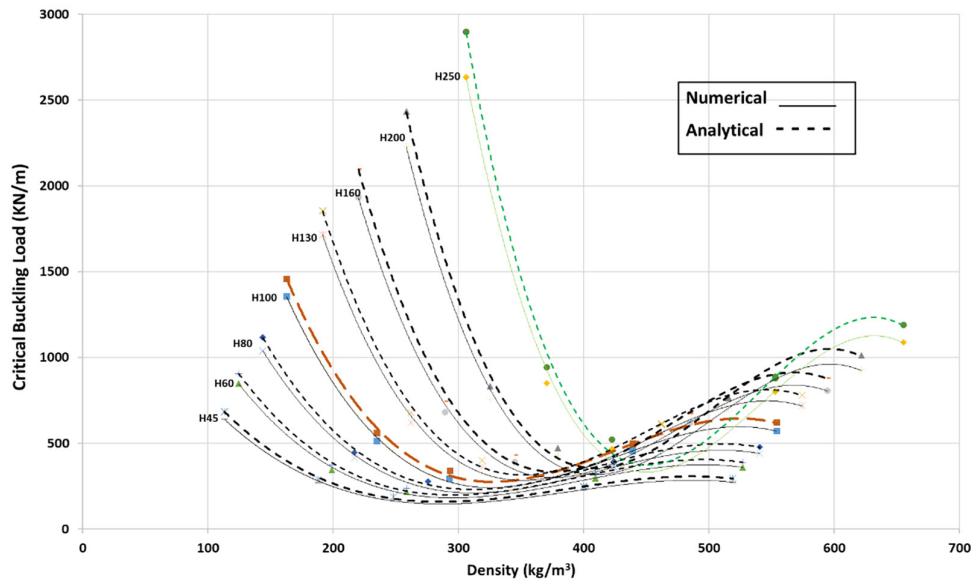**Figure 9.** Results for different plate form ratios

Figure 10. Change in critical buckling loads depending on core densities

It is clearly seen that the software developed in this study based on the LSPM is an effective tool for obtaining critical buckling loads in a shorter time than the commercial software based on FEM. By using this tool, the economy in time, labor, and budget can be provided while studying long sandwich plate optimization.

Footnotes

Authorship Contributions

Concept/Design: E. Altunsaray, and G. Neşer, Data Collection or Processing: E. Altunsaray, Analysis or Interpretation: E. Altunsaray, and G. Neşer, Literature Review: E. Altunsaray, Writing, Reviewing and Editing: G. Neşer.

Conflict of Interest: No conflict of interest was declared by the authors.

Financial Disclosure: The authors declared that this study received no financial support.

5. References

[1] S. Rudan, and L. Drobilo, "NFEM analysis of a composite made hull of autonomous underwater submersible", *Brodogradnja,* vol. 65, no. 3, pp. 101-115, 2014.

[2] F. Dominguez, and L. Carral, "A review of formulations to design an adhesive single-lap joint for use in marine applications", *Brodogradnja*, vol. 71, no. 3, pp. 89-118, 2020.

[3] J. G. Kang, M. C. Kim, I. R. Shin, and W. S. Jin, "Feasibility study on effect of structural flexibility of asymmetric pre swirl stator on propulsion performance for Kriso Container Ship(KCS)", *Brodogradnja*, vol. 72, no. 4, pp. 103-119, 2021.

[4] M. Calvario, Z. Li, and C. G. Soares, "Buckling strength of a composite material wave energy converter structure under slamming loads", *Ocean Engineering*, vol. 241, pp. 110044, 2021.

[5] M. Li, R. Yan, W. Shen, K. Qin, J. Li, and K. Liu, "Fatigue characteristics of sandwich composite joints in ships", *Ocean Engineering*, vol. 254, pp. 111254, 2022.

[6] E. P. Bilalis, M.S. Keramidis, N.G. Tsouvalis, "Structural design optimization of composite materials drive shafts", *Marine Structures*, vol. 84, pp. 103194, 2022.

[7] COReS, Best Practice Guide for Sandwich Structures in Marine Applications, 279.2013.

[8] V. Birman and G.A. Kardomateas, "Review of current trends in research and applications of sandwich structures", *Composites Part B: Engineering,* vol. 142, pp. 221-240, 2017.

[9] A. M. Zenkour, and M. Sobhy, "Thermal buckling of various types of FGM sandwich plates", *Composite Structures*, vol. 93, no. 1, pp. 93-102, 2010.

[10] M. A. Al-Shammari, and M. Al-Waily, "Analytical investigation of buckling behavior of honeycombs sandwich combined plate structure", *International Journal of Mechanical and Production Engineering Research and Development*, vol. 8, no. 4, pp. 803-818, 2018.

[11] M. A. Torabizadeh, "Buckling of the composite laminates under mechanical loads with different layups using different plate theories". *Advanced Composites Letters*, vol. 24, no. 1, pp. 12-20, 2015.

[12] R. Vescovini, M. D'Ottavio, L. Dozio, and O. Polit, "Buckling and wrinkling of anisotropic sandwich plates". *International Journal of Engineering Science*, vol. 130, pp. 136-156, 2018.

[13] S. Wang, et al. "Buckling analysis of hybrid fiber-reinforced composite sandwich panels with varying numbers of polyurethane cores", *Polymer Composites*, vol. 45, no. 16, pp. 15062-15085, 2024.

[14] H. Qian, et al. "Buckling analysis of sandwich plates reinforced with various loading of multi-walled carbon nanotubes", *Engineering Structures,* vol. 294, pp. 116765, 2023.

[15] L. He, A. Maalla, X. Zhou, and H. Tang, "Buckling and post-buckling of anisogrid lattice-core sandwich plates with nanocomposite skins", *Thin-walled Structures,* vol. 199, pp. 111828, 2024.

[16] V. M. Anh, N. D. Dat, and N. D. Duc, "Buckling and post-buckling of sandwich plate with functionally graded graphene origami reinforced core layer in hygrothermal environment", *VNU Journal of Science: Mathematics – Physics,* vol. 39. no. 4, pp. 14-25, 2023.

[17] G. D. Cara, M. d'Ottavio, and O. Polit, "Variable kinematics finite plate elements for the buckling analysis of sandwich composite panels", *Composite Structures,* vol. 330, pp. 117856, 2024.

[18] L. P. Kollar, and G. S. Springer, *Mechanics of composite structures,* Cambridge University Press, NY, USA, 2003.

[19] e. Altunsaray, "Parametric study of buckling of long sandwich rectangular plates". In *Proceedings of the 3rd International Congress on Engineering, Architecture and Design*, Kocaeli, Türkiye, May 04-05, 2018.

[20] ANSYS Academic, 2024R2.

[21] DiabGroup, "Divinycell H - Excellent mechanical properties to low weight", Accessed: Sep. 2024. [Online]. Available: https://www.diabgroup.com/products-services/divinycell-pvc/divinycell-h